coatings

MDPI

Article

Anti-Graffiti Coatings on Stones for Historical Buildings in Turin (NW Italy)

Chiara Ricci [1,2,*], Francesca Gambino [1], Marco Nervo [1], Anna Piccirillo [1], Arianna Scarcella [1], Alessandra De Stefanis [1] and Jose Santiago Pozo-Antonio [2,3,*]

1   Fondazione Centro Conservazione e Restauro "La Venaria Reale", 10078 Venaria Reale (TO), Italy; francesca.gambino@unito.it (F.G.); marco.nervo@centrorestaurovenaria.it (M.N.); anna.piccirillo@centrorestaurovenaria.it (A.P.); arianna.scarcella@centrorestaurovenaria.it (A.S.); alessandra.destefanis@centrorestaurovenaria.it (A.D.S.)
2   Dpto. Enxeñaría dos Recursos Naturais e Medio Ambiente, Escola de Enxeñaría de Minas e Enerxía, Universidade de Vigo, 36310 Vigo, Spain
3   CINTEXC, Universidade de Vigo, 36310 Vigo, Spain
*   Correspondence: cricci@uvigo.es (C.R.); ipozo@uvigo.es (J.S.P.-A.)

check for updates

Abstract: The application of anti-graffiti products to stones belonging to architectural heritage is a common procedure that is currently complementary to traditional graffiti removal treatments, such as chemical and mechanical cleaning. In this study, two anti-graffiti coatings (a sacrificial product and a permanent one) were tested on four stones (with a different texture, mineralogy, and surface finish) commonly found in the historical city center of Turin (Italy). In order to evaluate the effectiveness of the anti-graffiti products, the removal of two graffiti paints with different compositions was tested. The results of the cleaning procedures performed on the surfaces coated with anti-graffiti products were evaluated, considering both the graffiti remains and the alterations induced on the surface. Chemical cleaning based on the use of a low-toxic ternary solvent mixture was applied on the unprotected stones for a comparison with the results obtained on the surfaces coated with anti-graffiti products. The samples were observed under stereomicroscopy and ultraviolet fluorescence photography and all of the treated surfaces were evaluated by roughness measurements, the contact sponge method, static contact angle measurements, and scanning electron microscopy. The composition of the anti-graffiti product, the graffiti paint to be cleaned, and the remover recommended by the manufacturer proved to be key factors for the cleaning effectiveness achieved on coated surfaces. Moreover, to a lesser extent, the mineralogy, texture, and surface finish of the stone also influenced the results of the cleaning procedures. The sacrificial anti-graffiti product enhanced the cleaning effectiveness on all stones if compared to uncoated surfaces; however, the permanence of coating remains on the surface after cleaning proved to be critical. Regarding the use of the permanent anti-graffiti products, intense disparate results were achieved, depending on the graffiti paint composition.

Keywords: anti-graffiti; spray graffiti; cultural heritage; granite; gneiss; diorite; travertine

1. Introduction

As Cultural Heritage is considered a driver and enabler of sustainability for the future by UNESCO [1], ICOMOS promotes scientific studies to enhance the conservation of tangible cultural heritage in the framework of sustainable cities and tourism [2].

In the last few years, scientific research on the cleaning of different types of deposits, patinas, and crusts from stones belonging to cultural heritage has been quite rich [1–5]. Considering that

graffiti has been one of the most serious threats to cultural heritage conservation in the last few decades, an important effort has been made to develop different cleaning methods. Recently, great interest has also been devoted to the application of anti-graffiti products, in order to avoid the drawbacks of traditional cleaning methods [6–11]. Indeed, although chemical cleaning products are among the cheapest solutions, they may penetrate the substrate and cause irreversible damage, such as chemical contamination, as well as ghosting, due to paint dissolution and its subsequent penetration into the substrate [4,12,13]. Furthermore, they represent a risk for the environment and the conservator-restorer's health. Regarding mechanical methods, despite also being low-cost cleaning methods, they can damage the stone, inducing mineral grain extraction or provoking cracks and fissures [14–16]. Moreover, beyond being expensive, more advanced systems, such as laser ablation, may also induce changes on the stones: the use of a laser may cause color modifications of the surface and mineralogical alterations, such as the melting of biotite and feldspar and cleavage fracture of quartz [17–20]. Recently, bioremediation for graffiti removal has been considered an interesting field with promising results, but is still being intensely researched [21,22]. Considering the cited drawbacks of other cleaning methods, the development of anti-graffiti coatings to protect stone surfaces and facilitate the removal of graffiti paints is justified. Making the procedures for the removal of graffiti simpler or limiting the effect of future defacing actions against Cultural Heritage may also generate benefits in terms of economic sustainability. Nowadays, there about 21 scientific papers on this topic, mainly focused on carbonate stones [5,11,23], while silicate stones have been less frequently studied.

Anti-graffiti products can be divided into two groups—sacrificial and permanent coatings—both of which are based on the creation of layers on the stone surface with a low surface energy, with the aim of reducing the interaction with graffiti paint [7,8,24,25]. Specifically, sacrificial products are generally composed of waxes, acrylates, and polysaccharides. They are removed with the graffiti paint layer and therefore need to be reapplied after every cleaning process. Permanent anti-graffiti coatings are generally composed of polyurethanes, fluorocarbon, and alkyl alkoxy silanes; those products are supposed to hinder the adhesion of the graffiti paint layer to the stone surface and to make its removal easier [7,25]. Moreover, permanent anti-graffiti coatings are characterized by a longer durability and should be resistant to several repeated cleaning cycles [5,23,26–29].

In [5] and [28], the most important features of anti-graffiti coatings to be applied on historical buildings and monuments are summarized as transparency, a low surface energy, durability under outdoor conditions, reversibility by means of mild cleaning systems, permeability to water vapor, and water repellence. However, in order to achieve satisfactory cleaning levels, other aspects related to the stone must be taken into consideration, such as the porosity and the surface roughness [7,25]. Carmona-Quiroga et al. [7,25] found that the performances of two different permanent anti-graffiti products were higher when applied on limestone rather than on granite, due to the different finishes of the two stones, with the limestone being smoother than the granite. Similarly, Pozo-Antonio et al. [11] reported a study on the effectiveness of two commercial anti-graffiti coatings (one sacrificial and one permanent) applied on two granitic stones with different textures and compositions. These lithotypes were painted with two spray paints and then cleaned following the procedures recommended by the manufacturers. The chemical composition of the paints and the removal time were cited as the most relevant parameters to be considered. Recently, Macchia et al. [23] tested the use of permanent and sacrificial anti-graffiti coatings for the protection and maintenance of contemporary mural paintings from vandalism spray. They found that the anti-graffiti did not penetrate into the underlying paints and did not produce notable colorimetric alterations. They also found that the permanent anti-graffiti based on fluorinated acrylic polymers was the product providing the best performance.

García and Malaga [28] and, more recently, Grossi and Del Lama [26], described the tests and techniques which may be performed to assess the effectiveness and durability of anti-graffiti products, such as colour spectrophotometry and gloss measurements, scanning electron microscopy, static contact angle measurements, capillarity tests, assessments of water absorption under low pressure (pipe method), and water penetration (Karsten tube).

In this research, two anti-graffiti products (one sacrificial and one permanent) were applied on four stones with a different texture and mineralogy (a gneiss, granite, diorite, and travertine), with the most representative surface finish for the architectural heritage built in Turin (NW Italy). In order to evaluate the performance of each anti-graffiti paint, two graffiti paints with different compositions (one alkyd-based and one acrylic-based) were applied on coated stone surfaces, which were then cleaned with the products recommended by the manufacturer. The results obtained were compared with a chemical cleaning procedure applied on painted surfaces without anti-graffiti product. Specifically, a low-toxic solvent mixture was used, following Ricci et al. [30], taking into account the sustainability regarding the environment and safeguarding of human health, as well as the lowest impact on the original stone materials.

The treated surfaces were evaluated considering the graffiti remains and the alterations induced on the surface. The samples were observed under stereomicroscopy and ultraviolet fluorescence photography and all of the treated surfaces were also evaluated by roughness measurements, the contact sponge method, and static contact angle measurements. In order to determine the morphology and composition of the graffiti remains, as well as the remains of the anti-graffiti coatings after cleaning, the surfaces were evaluated with scanning electron microscopy.

2. Materials and Methods

2.1. Stones

Mainly due its geographical location and proximity to the Alps, around 50 different ornamental stones are present in the Historical and Modern Architecture of the city of Turin (NW Italy). As part of the research project "Degrado Urbano" carried out by Fondazione Centro Conservazione e Restauro "La Venaria Reale" (see the "Funding" section below), a preliminary survey was performed to map the lithotypes most affected by graffiti. The abundance of each stone in the city center and the surface finish were also considered: according to the literature [31–34], the largest number of stones employed for architecture are metamorphic (either gneiss or marbles), followed by magmatic (granites and granitoids) and sedimentary (travertines, limestones, and sandstones) stones. For this research, four representative stones were selected, taking into account their different mineralogy, structure, and color. Figure 1 shows digital photographs of the selected stones. Furthermore, Figure 2 shows micrographs of the stone surfaces captured with an OLYMPUS SZ ×10 stereomicroscope (Olympus Corporation, Shinjuku, Tokyo, Japan) with an OLYMPUS Color View I digital camera and FEI Quanta 200 scanning electron microscope (Thermo Fisher Scientific, Waltham, MA, USA) with energy-dispersive X-ray spectroscopy (SEM-EDX) in high-vacuum conditions and back scattered electron (BSE) mode. The optimum conditions of observation with SEM-EDX were obtained in high-vacuum conditions, at an accelerating potential of 15–20 kV, a working distance of 9–12 mm, and a specimen current of ~60 mA.
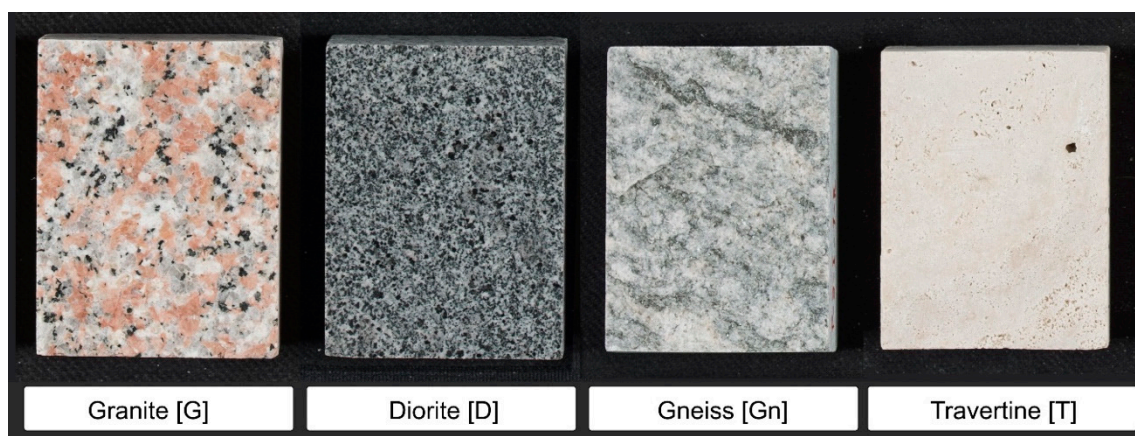

| Granite [G] | Diorite [D] | Gneiss [Gn] | Travertine [T] |

Figure 1. Digital photographs of the selected stone. Each stone shows the corresponding ID in brackets.
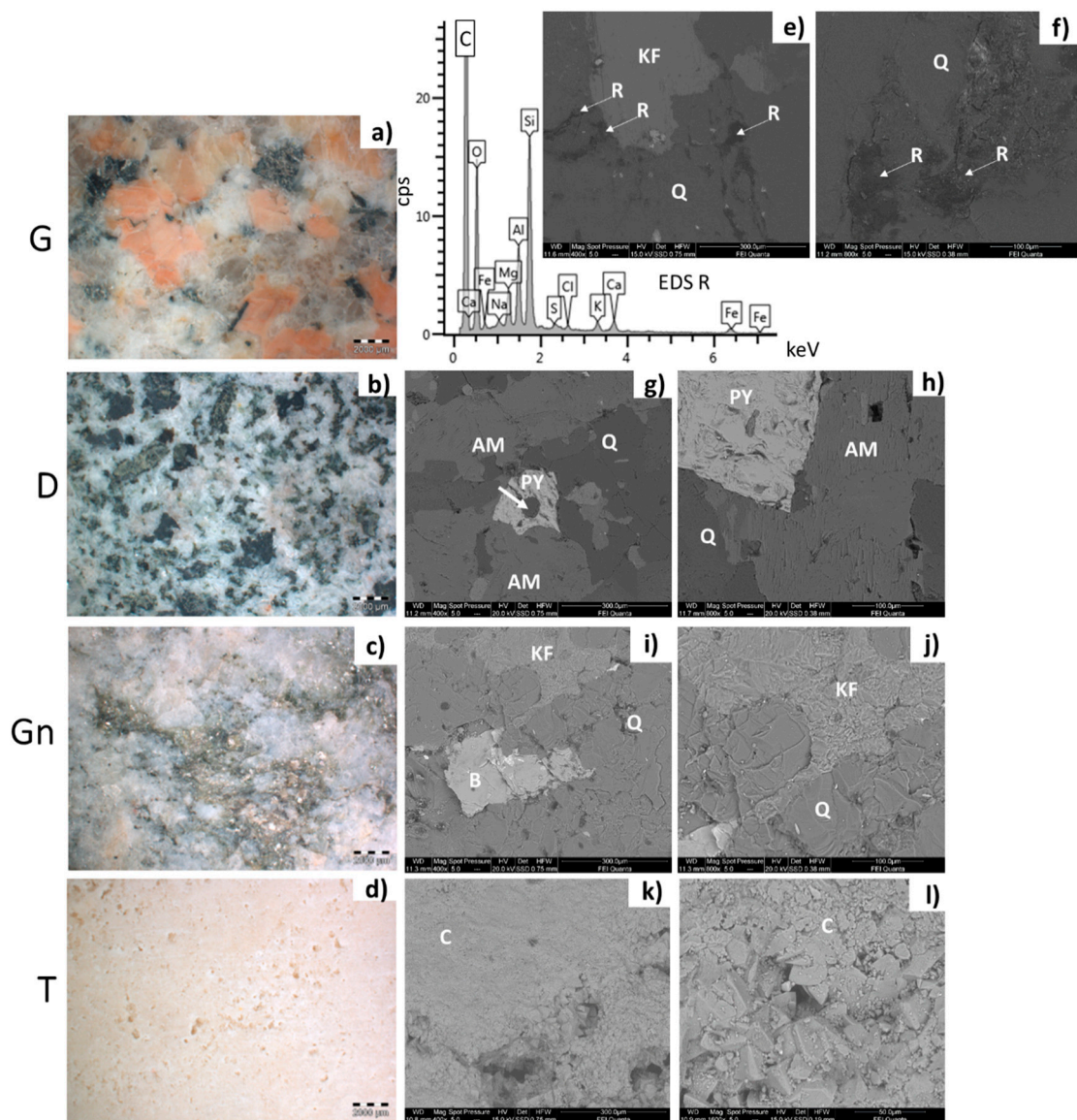
Figure 2. Micrographs taken with stereomicroscopy of the selected stones (**a–d**). SEM micrographs of the stones: granite (**e,f**), diorite (**g,h**), gneiss (**i,j**) and travertine (**k,l**). Granite micrographs (**e,f**) are accompanied by the EDX spectrum of the epoxy resin (R) used during the polishing treatment to fill the fissures. Q: quartz, AM: amphibole, PY: pyroxene; B: biotite, KF: potassium feldspar, and C: calcite.

The selected stones were as follows:

(1) Baveno granite (hereinafter G, Figures 1 and 2a,e,f), which is a medium-grained and pink granite, composed of white plagioclase, gray quartz, pink K-feldspar, and biotite partially replaced by chlorite [35,36]. It takes its name from the main quarry, located in the small town of Baveno on the west bank of Maggiore Lake (in the Verbano-Cusio-Ossola quarry district, northern sector of the Piedmont region) [31]. In Turin, it has been employed with both a polished and unpolished surface, depending on the application. Within this work, a polished surface finish was considered, as it occurs, for example, for several columns of the typical arcades in the city center. It is known that during the polishing process, an epoxy resin filler is used to fill any micro fissures [37]. The EDX spectra reported in Figure 2 highlight the presence of this resin on the granite (Figure 2e,f), showing C, Al, and Si as major elements and, to a lesser extent, Mg, Na, S, Cl, K, Ca, and Fe;

(2) Vico diorite (hereinafter D, Figures 1 and 2b,g,h) is a quartzdiorite with a granular texture and characterized by a light to very dark gray colour, depending on the grain size and the percentage of femic minerals, represented by amphibole, biotite, and rare pyroxene. With regards to sialic minerals, plagioclase mainly occurs, in addition to K-feldspar and rare quartz [38]. Vico diorite comes from the quarry district of the Chiusella Valley, which is about 70 km from Turin [31]. As for the granite, a polished surface was selected for the Vico diorite, as this surface type was observed for several columns and paving of the arcades of blocks in the city center. Si-rich fillers were detected in the superficial voids and fissures of this stone (as highlighted in Figure 2g with an arrow), as a result of the silicone-based chemical applied to enhance the absorption qualities, increase the resistance to staining, and/or alter the stone´s appearance [37];

(3) Luserna Stone (*Pietra di Luserna*, hereinafter Gn, Figures 1 and 2c,i,j) is an orthogneiss. It is named after the municipality of Luserna San Giovanni, which is about 65 km from Turin (NW Italy), where the main quarry district was historically located [31]. It is characterized by a micro-augen texture, medium-fine grained size, and good fissibility along the schistosity planes, well-defined by muscovite crystallized under high-pressure conditions [38]. It displays a light gray colour, occasionally turning slight darker or greenish; magmatic porphyroclasts of K-feldspar, in addition to quartz and albite, are clearly visible. As for the forming minerals, it is composed of quartz, plagioclase, K-feldspar, muscovite, and biotite; epidote, chlorite, and sphene are also present as minor minerals [32]. Luserna Stone has been frequently employed in Turin, such as in the case of the slabs of the dome of the Mole Antonelliana (a major landmark building in the city) and the façade of the Automobile Museum. As for numerous real applications, a flamed surface finish was considered for this stone within the present work;

(4) Travertine (hereinafter T, Figures 1 and 2d,k,l) is a very porous orthochemical sedimentary rock, with fine grains. It is completely composed of a calcite matrix and often contains plant prints. Macroscopically, it is characterized by a more or less intense beige color, with thin bands highlighted by different contents of impurities [39]. Among the four lithotypes selected, it is the only one not from the Piedmont region, with the main mining area being located in the region of Rome [31]. Nevertheless, it was included in the present work since it has been frequently employed in Turin, such as in the case of the façade and arcades of the Santissima Annunziata church, as well as several façades of buildings and shops in the city center. As is mostly seen in Turin, a smooth disc-cutting finish was selected for the travertine.

Seven slabs of 5 cm × 5 cm × 2 cm were obtained for each stone.

2.2. Anti-Graffiti Products

Four slabs of each stone were coated with anti-graffiti commercial products; specifically, two slabs were coated with a sacrificial anti-graffiti and two with a permanent anti-graffiti product. Both anti-graffiti products were applied with a brush, following the instructions provided by the manufacturers in the data sheets and avoiding localized accumulations of the coating.

The selected sacrificial anti-graffiti product is called ISOGRAFF, provided by Colorificio San Marco Spa (Marcon VE, Italy) which is a ready-to-use commercial product composed of an aqueous dispersion of microcrystalline wax, with pH 6–6.5 (as reported in the technical data sheet, [40]). Two layers of coating were applied 20 min apart.

The permanent anti-graffiti, COLORDOC PLUS ANTI-GRAFFITI provided by Docchem srl (Dorno PV, Italy), is a fluorinated polyurethane in a water emulsion, with pH 7. It is a bicomponent product whose polymeric component has to be blended with the crosslinker component diluted to 100:10 (*w/w*) (as reported in the technical data sheet, [41]). Two layers of coating were applied in orthogonal directions, 4 h apart.

2.3. Graffiti Paints and Application

Two graffiti paints from MONTANA Colors [42] with different compositions were used: a violet spray paint, the MTN94 Ultraviolet RV173, and a green dabber paint, the MTN Street Paint Dabber UFO Green.

These graffiti paints were previously used in [30]: the violet paint exhibits an alkyd organic base, while the green paint is an acrylic modified with styrene. The inorganic component of the paints investigated by XRF showed the presence of Ti, Si, Cl, Ca, S, and Al for both paints [30]. Other chemical elements were found: Fe, Co, P, and K in the violet spray paint and Cu in the green dabber paint [30].

In the case of the violet paint, the surfaces were sprayed for 3 s at an angle of 45° and from a distance of about 30 cm, following [17]. The green paint was applied by means of a high flow dripper/squeezer marker. After the application of the paints, samples were left to air-dry (20 ± 2 °C and 50 ± 10% RH) in laboratory conditions for seven days.

Both the violet and green graffiti paints were applied on three slabs of each stone: (i) one coated with the sacrificial anti-graffiti product; (ii) one coated with the permanent anti-graffiti product; and (iii) one without any anti-graffiti coating.

Samples were then left for 3 months outdoors for natural aging.

2.4. Cleaning

Samples were cleaned using the corresponding remover. It has to be highlighted that these graffiti removers are commercial ready-to-use products and thus may be employed by non-expert users.

Therefore, the GRAFFITI REMOVER by Colorificio San Marco Spa was used for samples coated with the sacrificial anti-graffiti ISOGRAFF. To overcome the lack of information about the chemical composition of the product in the technical data sheets provided by the manufacturer, a Fourier-transform infrared spectroscopy (FTIR) analysis was performed with an FT-IR Bruker Vertex 70 (Bruker, Billerica, MA, USA). This allowed the identification of a mixture of alkyl carbonate, ethyl pyrrolidone, alcohol ethoxylates, and possibly dimethyl adipate as cleaning agents, combined with cellulose ether polymers as thickening agents. This product was supposed to solubilize the microcrystalline wax-based coating, allowing its removal from the stone surface, together with the graffiti paint.

Alternatively, to clean the samples coated with the permanent anti-graffiti COLORDOC PLUS ANTI-GRAFFITI, the specific remover REMOGRAFFIDOC F8 by Docchem srl (Dorno PV, Italy) was used. It was supposed to remove the graffiti paint layer, without interaction with the protective coating. As in the previous case, the technical data sheet did not provide detailed information about the chemical composition, reporting the presence of undefined solvents and non-ionic and anionic surfactants. FTIR analysis allowed us to identify the presence of a blend of alcohol and terpene solvents.

Both commercial anti-graffiti removers were used as indicated in the data sheet: they were applied directly on the stone surface with a brush, left to soak for a few minutes, and then removed with a dry paper towel and the sample surface was finally rinsed with a wet sponge.

For comparative purposes, uncoated surfaces (without anti-graffiti product) painted with the same graffiti paints were cleaned with one low-toxic ternary solvent mixture (either mixture A or B) specifically formulated and composed of ethyl alcohol, acetone, and isooctane (2,2,4-trimethylpentane), in different concentrations (% *v/v*). The two ternary solvent mixtures were designed to replace either the use of methyl ethyl ketone (MEK) or n-butyl acetate. In fact, both MEK and n-butyl acetate are used for cleaning treatments in the field of the conservation of Cultural Heritage and have been proven to be the most effective, among other common pure solvents or solvent blends, for the removal of the considered graffiti paints [13]. However, they are characterized by a relevant toxicity, as shown by their Threshold Limit Value-Time-Weighted Average (TLV-TWA) values, which are 50 and 200 ppm, respectively [43]. The TLV-TWA represents a measure of the maximum amount of solvent that a worker can be safely exposed to on a daily basis for a working life (8 h/day, 40 h/week work schedule), e.g., for n-butylacetate, a worker can be safely exposed to 50 ppm of this product on a

workable day (8 h/day). With the aim of using more sustainable cleaning products, alternative ternary mixtures composed of solvents with a lower toxicity were formulated using the open source software Trisolv® [44], developed by the Istituto Superiore per la Conservazione ed il Restauro" (ISCR) and based on the triangular Teas graph [45,46]. Therefore, keeping the same solubility parameters, n-butyl acetate was replaced with a mixture (hereinafter called "mixture A") of 51% ethyl alcohol, 11% acetone, and 38% 2,2,4-trimethylpentane, while MEK was replaced by a mixture (hereinafter called "mixture B") of 7% ethyl alcohol, 80% acetone, and 13% 2,2,4-trimethylpentane. It has to be highlighted that the formulation and use of these mixtures requires technical expertise and they should thus be employed by professional conservators/restorers. Both mixture A and B were applied on the painted surface of the slabs by means of a small cotton swab. A Japanese paper layer was interposed, in order to reduce the solvent penetration and evaporation, thus preventing excessive paint dissolution and ghosting and health risks for the restorer as much as possible. After 1 week at room conditions, during which the samples dried at a constant mass, stereomicroscopy was used to identify the paint remains on the surface: based on this evidence, the ternary solvent mixture providing the best performance for each paint–stone pair was selected. In particular, regardless of the paint composition, mixture A was selected for granite and gneiss samples and mixture B for diorite and travertine.

The samples used in this research are detailed in Table 1, where the ID for each sample is also shown.

Table 1. Samples used in this research. Identification (ID) for each sample is also provided.

Stone	Paint Layer	Description	ID
Granite	–	Reference stone	G
	–	Sacrificial anti-graffiti	GS
	–	Permanent anti-graffiti	GP
	Violet	Solvent mixture A	GVSa
		Sacrificial anti-graffiti	GVS
		Permanent anti-graffiti	GVP
	Green	Solvent mixture A	GGSa
		Sacrificial anti-graffiti	GGS
		Permanent anti-graffiti	GGP
Diorite	–	Reference stone	D
	–	Sacrificial anti-graffiti	DS
	–	Permanent anti-graffiti	DP
	Violet	Solvent mixture B	DVSb
		Sacrificial anti-graffiti	DVS
		Permanent anti-graffiti	DVP
	Green	Solvent mixture B	DGSb
		Sacrificial anti-graffiti	DGS
		Permanent anti-graffiti	DGP

Table 1. *Cont.*

Stone	Paint Layer	Description	ID
Gneiss	–	Reference stone	Gn
	–	Sacrificial anti-graffiti	GnS
	–	Permanent anti-graffiti	GnP
	Violet	Solvent mixture A	GnVSa
		Sacrificial anti-graffiti	GnVS
		Permanent anti-graffiti	GnVP
	Green	Solvent mixture A	GnGSa
		Sacrificial anti-graffiti	GnGS
		Permanent anti-graffiti	GnGP
Travertine	–	Reference stone	T
	–	Sacrificial anti-graffiti	TS
	–	Permanent anti-graffiti	TP
	Violet	Solvent mixture B	TVSb
		Sacrificial anti-graffiti	TVS
		Permanent anti-graffiti	TVP
	Green	Solvent mixture B	TGSb
		Sacrificial anti-graffiti	TGS
		Permanent anti-graffiti	TGP

2.5. Analytical Techniques

The surfaces coated with anti-graffiti products and the treated surfaces after cleaning with the products recommended by the manufacturer and the low-toxic ternary solvent mixture were inspected using the following analytical approach:

(1) The coated surfaces were observed with an OLYMPUS SZ ×10 stereomicroscope, with an OLYMPUS Color View I digital camera, in order to observe any visible effect of the anti-graffiti product applied on the different stones. Moreover, all surfaces, after having been treated with the different cleaning methods, were evaluated by stereomicroscopy to identify the graffiti remains. Moreover, in order to determine the thickness of the anti-graffiti coatings and the graffiti paints, fragments of 1 cm × 1 cm × 1 cm were embedded in resin to be visualized by means of stereomicroscopy;

(2) The water absorption of both the coated surfaces and the surfaces, after having been treated with the different removers, was evaluated by the contact sponge method. A CTS contact sponge kit was used, following [47]. It is a non-destructive water absorption test, which may be performed in both the laboratory and in situ and has been proven to be directly comparable with other water uptake laboratory measurements (e.g., the capillary rise method) [48]. A Spontex1 Calypso-type sponge, in natural fibers, having pre-determined characteristics and dimensions, was charged with an adequate amount of water (2 mL within the present work), after preliminary tests to verify that the water did not leak when the sponge was put in contact with the surface. The sponge was applied on the stone sample surface for 180 s, by using a Falcon 1034 Rodac® circular plastic plate: by placing the borders of the plate in contact with the examined surface, the maximum applicable manual pressure was determined. The amount of water absorbed by the surface was calculated by the difference, by weighing the sponge before and after the application. The difference in weight corresponds to the amount of water which has been absorbed by the material through the surface. The results (water absorption, *Wa*) were then expressed by the mass difference as a

function of area and time. For each surface, three measurements were performed, by drying the sample between measurements;

(3)   The hydrophobicity of the surfaces after cleaning was evaluated by means of a SEO Phoenix-300 Touch goniometer (Surface Electro Optics Co., Suwon, Korea) following BS [49] by applying the sessile drop method. Three drops of 6 μL of deionized water per sample were applied;

(4)   The variation of roughness of the surfaces after having been treated with the different cleaning methods were evaluated using a PLu 2300 Sensofar® optical imaging profiler (Sensofar, Barcelona, Spain). The images with the optical imaging profiler were collected with an EPI 10X-N objective, an overlap of 25%, a depth range of 2 mm, and a lateral resolution of 1 nm. The system allowed us to obtain 3D images of the cleaned surfaces and therefore, the roughness parameter ([50]), R_{3z} (third maximum peak-to-valley height), was obtained using the Gwyddion 2.47 software. For each sample, three images of 4 mm × 4 mm areas were taken and used to obtain the roughness parameter;

(5)   A microscopic evaluation of the cleaned surfaces was performed using a scanning electron microscope (FEI Quanta 200) in BSE mode to find the location of the graffiti and anti-graffiti remains and the damage induced on the surfaces. The optimal conditions of observation were the same as used to characterize the paint layers on the stone.

3. Results

After the application of the anti-graffiti coatings (Figure 3), different effects were observed, depending on the product used. For the sacrificial anti-graffiti product, visible changes were not observed in the silicate stones (granite, gneiss, and diorite, D and DS in Figure 3), while in the travertine, a glossy layer filling the typical voids of the stones was detected (T and TS in Figure 3). However, the permanent anti-graffiti product created a milky layer on the surface of the silicate stones, mainly visible on the diorite (D and DP in Figure 3). In the case of travertine, as for the sacrificial product, the accumulation of permanent anti-graffiti product was detected in the voids (T and TP in Figure 3).

Observations by stereomicroscopy of the cross sections of the anti-graffiti-coated surfaces with both paints allowed the identification of different thicknesses for both anti-graffiti products and paints. In general terms, the sacrificial anti-graffiti coatings showed a thickness lower than 10 μm, while the permanent anti-graffiti layers had a greater thickness, c.a. 15–50 μm. Moreover, the violet paint was a little thicker (c.a. 20–50 μm) than the green one (c.a. 5–15 μm). In Figure 3, micrographs of the cross sections from granite samples GVS and GGP are shown.

All surfaces corresponding to the different cleaning methodologies were evaluated by using stereomicroscopy (Figure 4). For all stones painted with the green graffiti, it was detected that, regardless of the composition of the anti-graffiti, the preliminary application of a protective coating on the stone surface (Figure 4 GGS, GGP, DGS, DGP, GnGS, GnGP, TGS, and TGP) enhanced the graffiti removal effectiveness, if compared to the cleaning conducted with the lox-toxic solvent mixture on the unprotected substrate (Figure 4 GGSa, DGSb, GnGSa, and TGSb). Unexpectedly, for samples painted with the violet spray, the presence of the permanent anti-graffiti coating on the surface made the extraction of the graffiti paint impossible (Figure 4, GVP, DVP, GnVP, and TVP).

Regardless of the chemical composition of the paint, in no case did cleaning by means of the ternary solvent mixtures achieve the complete removal of graffiti (Figure 4), with the worst results being respectively obtained for the gneiss and travertine. On the former, graffiti remains were detected in fissures and cracks associated with the flamed surface finish (Figure 4, GnGVs and GnGSa), while on the latter, remains were found in the typical voids of the stone (Figure 4 TVSa and TGSb). Conversely to the gneiss and travertine, for the polished samples (granite and diorite, respectively cleaned with mixture A and mixture B) (Figure 4 GVSa, GGVSa, DVSb, and DGSb), a lower amount of graffiti was found. The paint remains were mainly detected in the transgranular, intergranular, and intragranular fissures (characteristic features of these silicate stones, [51]), inducing the well-known ghosting effect [13].

Barely visible differences were observed, depending on the graffiti paint: a slightly higher amount of remains was detected for the green paint, if compared to the violet spray.
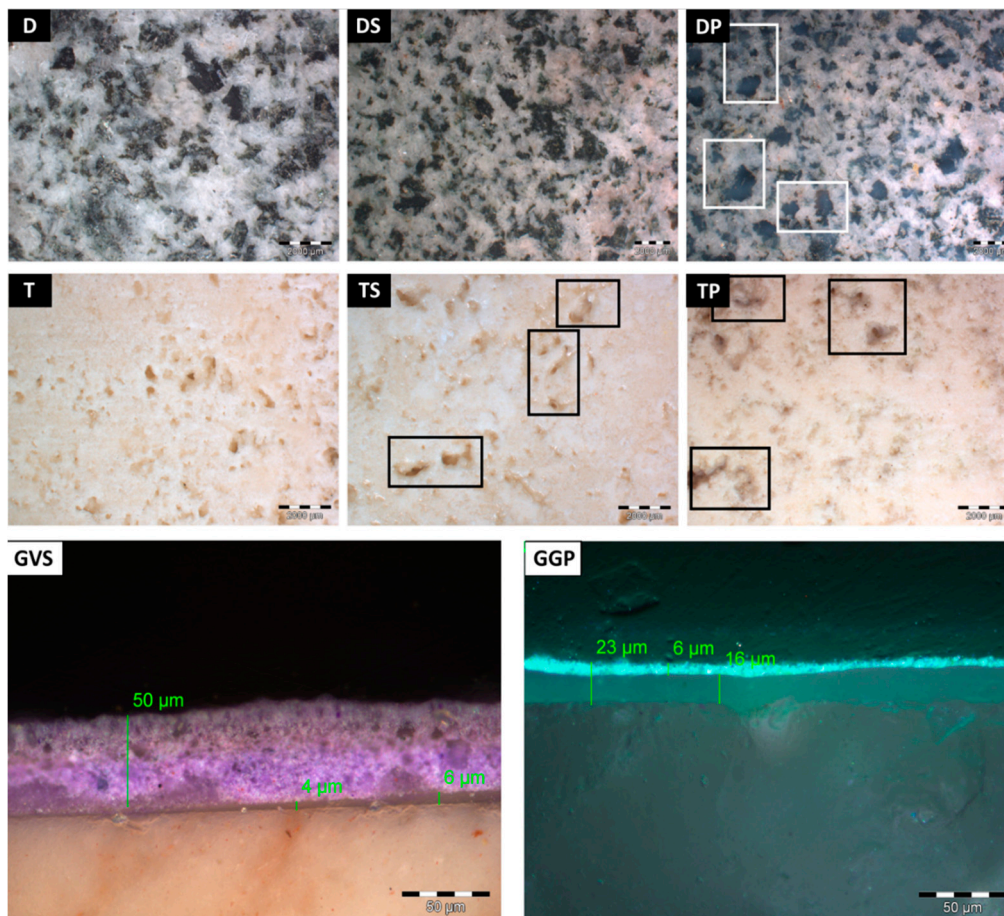

Figure 3. Micrographs captured by the stereomicroscopy of stones tested with both anti-graffiti sacrificial and permanent products. Moreover, micrographs of cross sections are provided (GVS and GGP), in order to show the thickness of the anti-graffiti coatings and paint layers. Check Table 1 for sample labeling.

With regard to the samples coated with the sacrificial anti-graffiti product, satisfactory graffiti removal was achieved for the silicate stones, in particular for those with a polished surface (i.e., granite and diorite, Figure 4 GVS, GGS, DVS, and DGS), for which a single wipe with the remover was already effective. Only a few isolated traces of paint were found on the granite; moreover, after the cleaning of the green paint from granite (Figure 4 GGS), the surface exhibited several white deposits. Overall, no clearly visible remains of graffiti filling the fissures were observed by stereomicroscopy on both granite and diorite.

For the samples with an unpolished surface, i.e., both the Luserna Stone (Figure 4 GnVS and GnGS) and the travertine (Figure 4 TVS and TGS), two to three wipes with the remover product were necessary for the cleaning. This occurred, in particular, for the violet spray paint, for which no effect was recorded with only a wipe of the remover; however, repeated steps finally resulted dissolution of the layer composed of both the protective coating and the graffiti. Few paint remains, regardless of the color and chemical composition, were found on the flamed gneiss surfaces (Figure 4 GnVS and GnGS), while in the case of travertine, the penetration of the graffiti paint into the voids of the stone hindered the evaluation of the cleaning effectiveness (Figure 4 TVS and TGS).
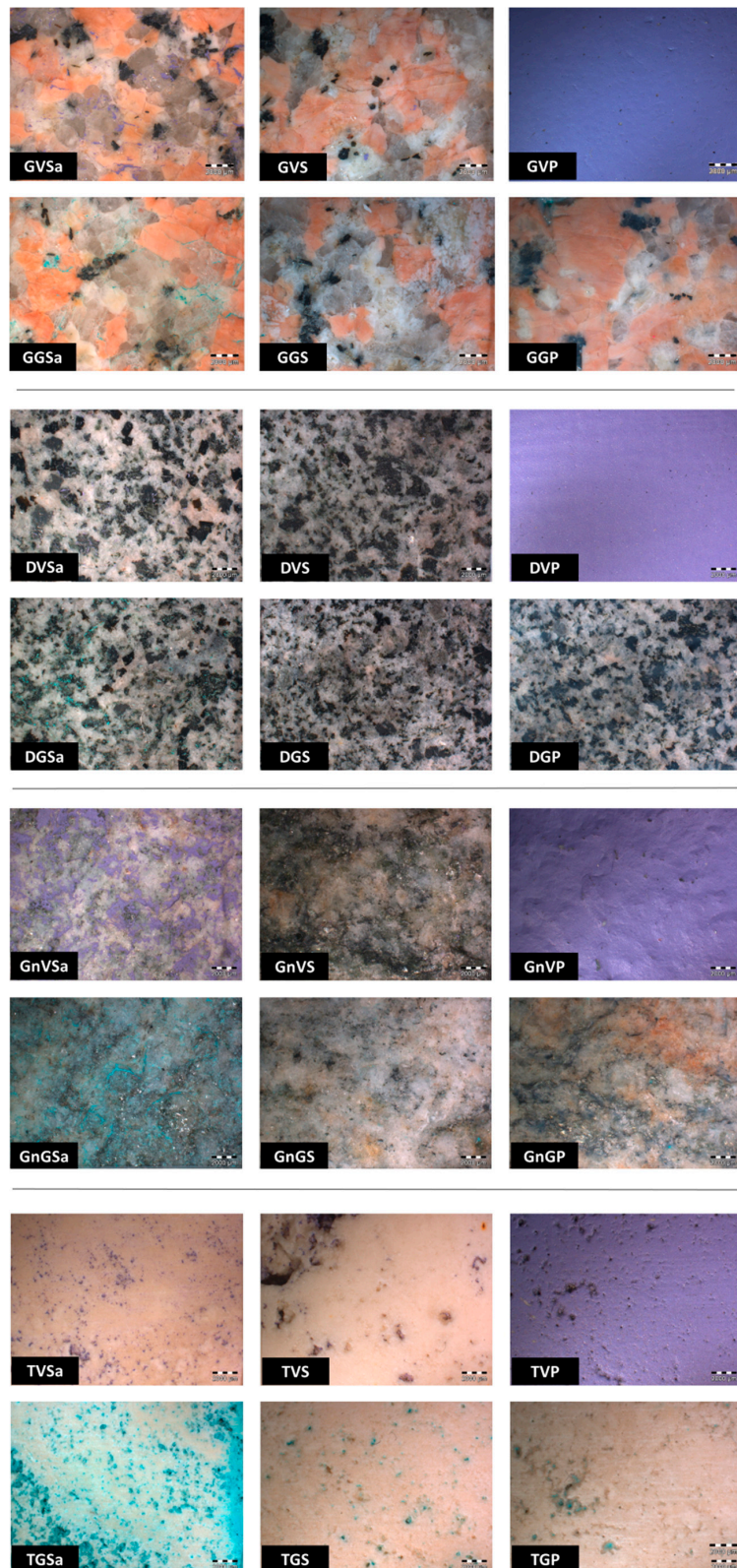
Figure 4. Micrographs taken by stereomicroscopy of the surfaces coated with anti-graffiti product after being cleaned with the products recommended by the manufacturers and the surfaces cleaned with the low-toxic ternary mixture. Check Table 1 for sample labeling.

Taking into consideration the surfaces coated with the permanent anti-graffiti product, disparate results were obtained, depending on the paint. For the green paint, (i) satisfactory graffiti removal was achieved for the granite and diorite (Figure 4 GGP and DGP), while (ii) on the gneiss and travertine, remains were detected in fissures and voids (Figure 4 GnGP and TGP). A greater amount of attention was devoted to the cleaning results obtained for samples painted with the violet graffiti: as already mentioned above, for all stones, the application of the commercial remover did not allow the removal of the paint layer from the surface (Figure 4 GVP, DVP, GnVP, and TVP), thus suggesting an interaction between the graffiti and the permanent protective coating, which determined the formation of a single thick and insoluble layer.

Although often not clearly visible with the observation made by the stereomicroscope, images captured with ultraviolet fluorescence photography allowed us to verify the presence of anti-graffiti coatings on the stone surfaces after the application of cleaning treatments. In Figure 5, digital UV-photographs of the gneiss samples coated with each anti-graffiti coating and after the application of the coupled commercial graffiti remover are shown. In the case of samples coated with the sacrificial anti-graffiti product, the presence of widespread remains of the product on the surface obviously represents a serious drawback (Figure 5 GnGS): indeed, the protective layer should be completely removed, together with the paint, after each cleaning treatment.
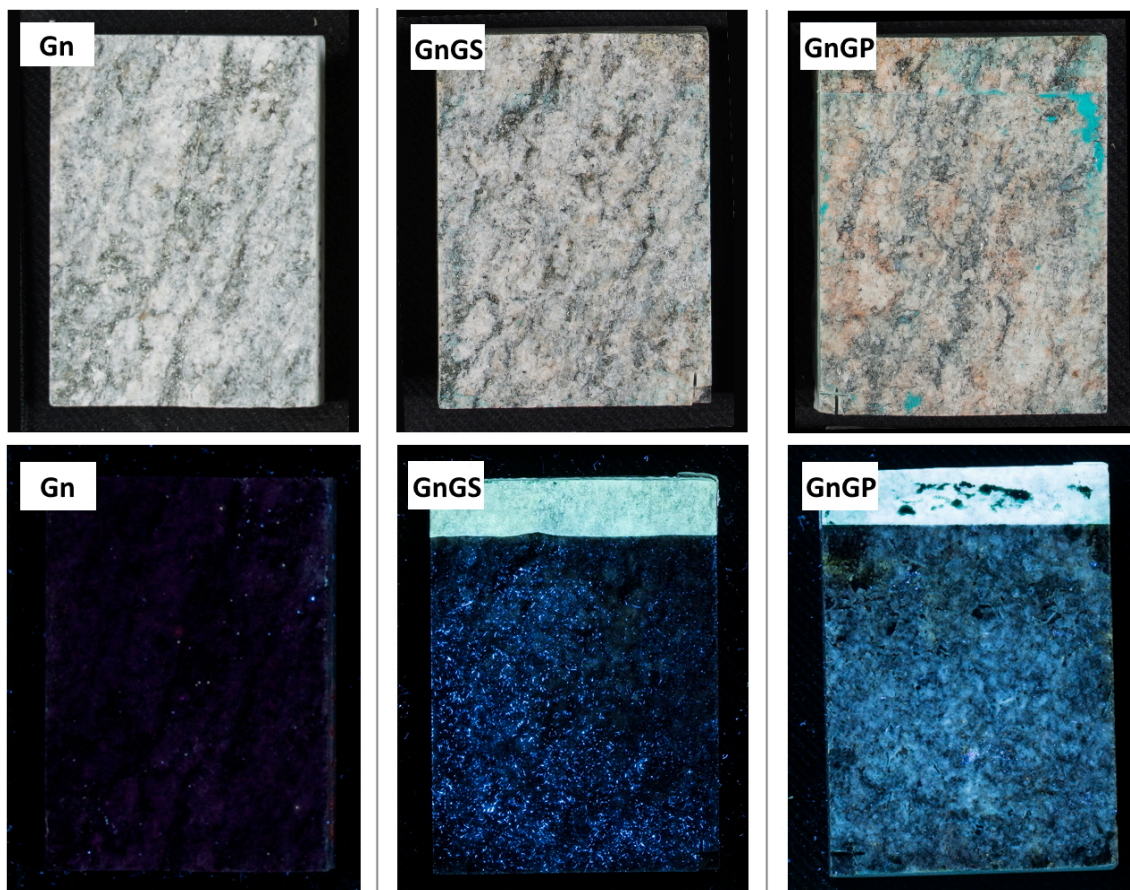

Figure 5. Digital and Ultraviolet (UV) photographs of the gneiss coated with the sacrificial and permanent anti-graffiti products after being cleaned with the products recommended by the manufacturers. Check Table 1 for sample labeling.

As for the permanent anti-graffiti product, it was observed that, even when persisting on the stone surface after cleaning, the protective layer showed gaps and discontinuities after one single application of the remover (Figure 5 GnGP). This pointed out a performance of the product quite different from

what was expected, since the protective layer created by a permanent anti-graffiti product should usually last for up to 10 cleaning cycles. Furthermore, this represents a risk for the substrate, since the graffiti paint partially solubilized by means of the remover may penetrate and induce stains on the stone surface.

As for the roughness of the samples, measurements of the parameter R_{3z} (third maximum peak-to-valley height) were performed on the cleaned surfaces, as well as on the reference stones for comparative purposes (Figure 6, Table S1). Considering the latter, it was observed that the granite and diorite (Figure 6, Table S1-G, D) displayed values similar to each other (around 2.30 μm), whose average was lower than the values detected for gneiss (33.7 ± 10.28 μm, Figure 6, Table S1-Gn) and travertine (5.23 ± 1.29 μm, Figure 6, Table S1-T). As obviously expected within this study, the highest R_{3z} value was obtained for the gneiss.
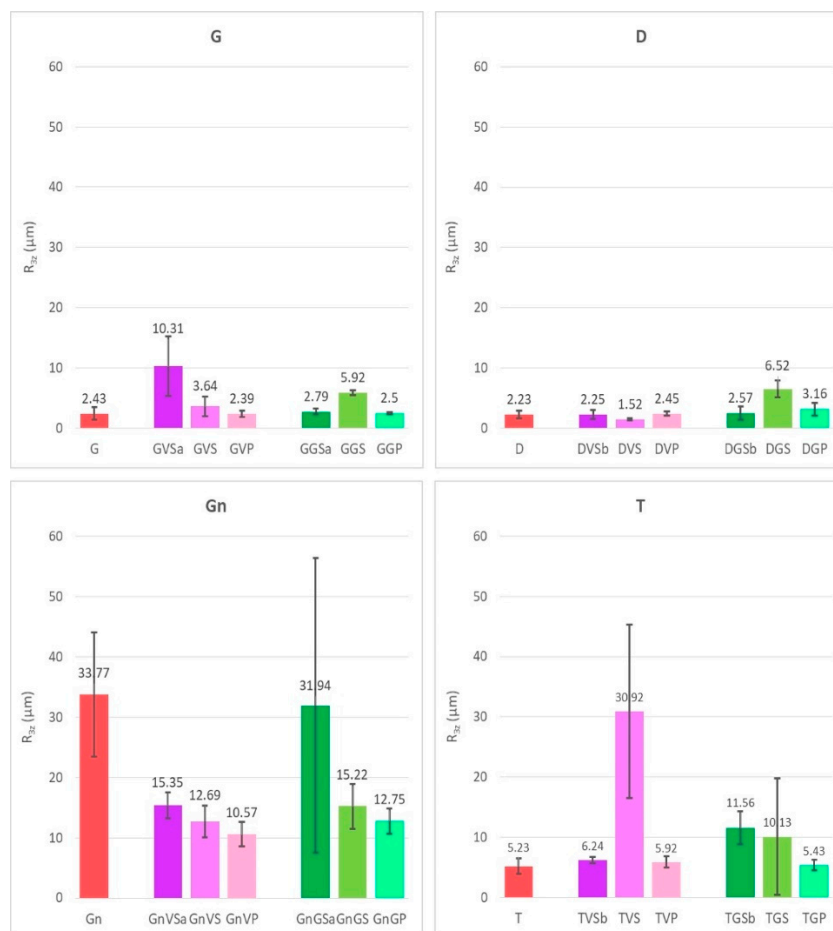
Figure 6. Roughness parameter R_{3z} of the uncoated stone and the surfaces coated with either the sacrificial or permanent anti-graffiti product after being cleaned with the respective products. *n* = 3. Standard deviation is also shown. Check Table 1 for sample labeling.

Furthermore, it was observed that the surfaces cleaned with the low-toxic ternary solvent mixtures usually exhibited an R_{3z} value similar to the values registered on the reference stones, except for a few cases: (i) the granite painted with violet spray (GVSa, R_{3z} = 10.31 ± 4.91 μm) showed a higher R_{3z} value than the reference (G); (ii) on the contrary, the gneiss with violet graffiti (GnVSa, R_{3z} = 15.35 ± 2.15 μm) exhibited a lower R_{3z} value than the reference (Gn); and (iii) similarly, the travertine with green graffiti (TGSb, R_{3z} = 11.56 ± 2.73 μm) displayed a higher R_{3z} value than the reference (T). The standard deviations computed proved that the differences between the reference and the exceptions were statistically different.

Considering the surfaces coated with the sacrificial anti-graffiti product, the granite, diorite, and travertine cleaned from green graffiti (Figure 6, Table S1-GGS, DGS, and TGS, respectively) demonstrated an increase of the roughness in comparison to the reference stones (Figure 6, Table S1-G, D, and T, respectively). For the travertine, a remarkable R_{3z} increase (almost a six-fold increase) was detected for samples cleaned from violet paint (Figure 6, Table S1-TVS). Conversely, the R_{3z} values measured for granite and diorite surfaces after the cleaning from violet graffiti (Figure 6, Table S1-GVS and DVS) were similar to those of the reference stones. Finally, for the gneiss, regardless of the paint, the roughness measured after the cleaning (Figure 6, Table S1-GnVS and GnGS) was considerably lower (a decrease of approximately 55%) than for the reference stone.

With regard to samples coated with the permanent anti-graffiti product, for those with a polished or smooth surface (G, D, and T), the R_{3z} values measured after cleaning were similar to those exhibited by the respective reference stones in all cases. Instead, regardless of the graffiti paint, the gneiss samples (Figure 6, Table S1-GnVP and GnGP) displayed a reduction of approximately 65% of the R_{3z} roughness after cleaning, if compared to the reference stone.

Taking into consideration the water absorption, Wa (Figure 7, Table S2), it was detected that among the uncoated surfaces, travertine (Figure 7, Table S2-T) showed the highest Wa (10.37 kg·s/m^2), while granite and diorite (Figure 7, Table S2-G, D) displayed the lowest values (~4.5 kg·s/m^2). It is important to highlight that the Wa of the travertine exhibited a high standard deviation (±5.3 kg·s/m^2), showing the influence of the characteristic voids of this stone on the measurement.
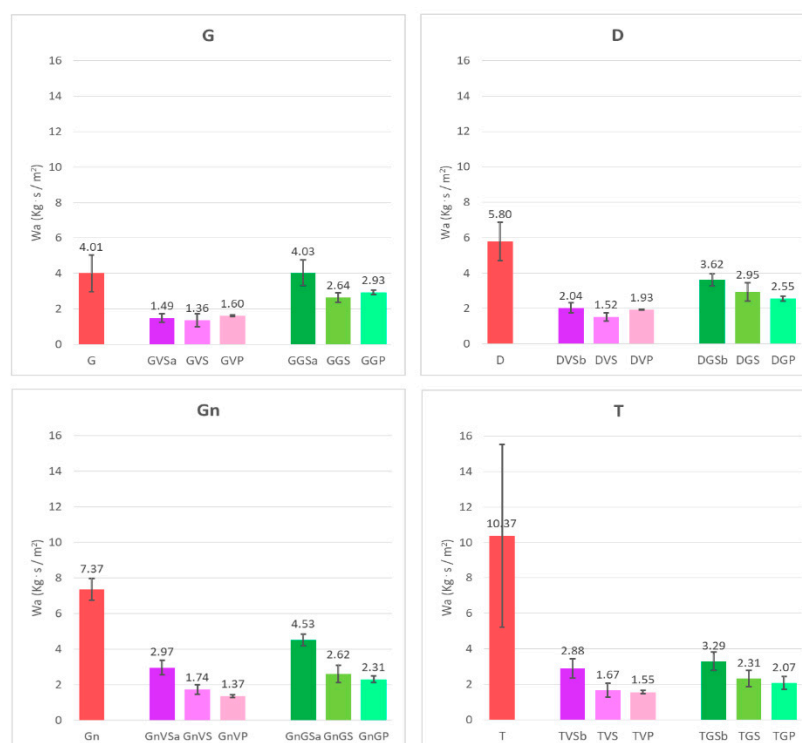

Figure 7. Water absorption (Wa, kg s/m^2) of the uncoated stone and the surfaces coated with either the sacrificial or permanent anti-graffiti product after being cleaned with the respective products. $n = 3$. Standard deviations are also shown. Check Table 1 for sample labeling.

After the cleaning, all surfaces (those uncoated and cleaned by ternary solvent mixtures-Figure 7, Table S2-GGSa, GVSa, DGSb, DVSb, GnGSa, GnVSa, TGSb, and TVSa, and those coated with both anti-graffiti products and cleaned with the coupled commercial removers-Figure 7, Table S2-GGS, GVS, GGP, GVP, DGS, DVS, DGP, DVP, GnGS, GnVS, GnGP, GnVP, TGS, TVS, TGP, and TVP) revealed lower

values of *W*a than the reference stones (Figure 7, Table S2-G, D, Gn, and T), being slightly lower for surfaces cleaned of violet graffiti.

For cleaning tests conducted by using the solvent mixture A or B (Figure 7, Table S2-GGSa, GVSa, DGSb, DVSb, GnGSa, GnVSa, TGSb, and TVSa), it was observed that, regardless of the stone, *W*a values lower than 3 kg·s/m^2 were obtained for samples with violet graffiti paint, while *W*a values lower than 4.6 kg·s/m^2 resulted from the green painted samples.

For the surfaces coated with the sacrificial anti-graffiti product (Figure 7, Table S2-GGS, GVS, DGS, DVS, GnGS, GnVS, TGS, and TVS), the water absorption was slightly lower than for the uncoated areas cleaned with the ternary solvent mixture, but in some cases, the differences were not statistically significant.

In the case of surfaces coated with the permanent anti-graffiti product (Figure 7, Table S2-GGP, GVP, DGP, DVP, GnGP, GnVP, TGP, and TVP), with the exception of the granite and diorite samples with violet paint (Figure 7, Table S2-GVP and DVP, respectively), the *W*a values were slightly lower than those found for the uncoated surfaces cleaned with the solvent mixture and the surfaces coated with the sacrificial anti-graffiti product, although these differences were not statistically significant in some cases.

Considering the hydrophobicity of the stones (Figure 8, Table S3), the four uncoated stones showed static contact angles (θ) lower than 90°; therefore, none of the original surfaces were hydrophobic [52]. The wetting behavior of a solid surface is driven by the surface free energy at the interfaces between the solid, liquid, and vapor [53].
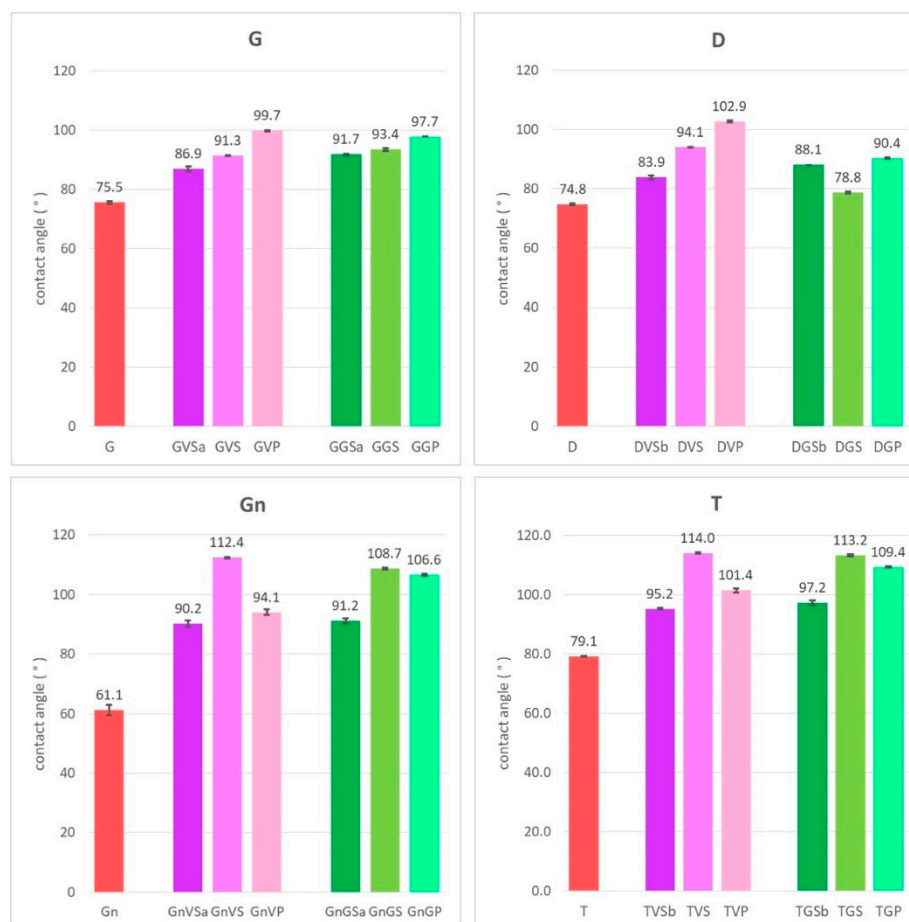

Figure 8. Static contact angle (θ°) of the uncoated stone and the surfaces coated with either the sacrificial or the permanent anti-graffiti product after being cleaned the respective products. *n* = 3. Standard deviations are also shown. Check Table 1 for sample labeling.

After cleaning, all of the coated surfaces showed higher contact angles than the references.

Overall, it is important to highlight that most of the treated surfaces exhibited static contact angles higher than 90°, showing hydrophobic behavior [52], with the exception of GVSa, DVSb, DGSb, and DGS, with three out of four of them being uncoated surfaces cleaned by using a ternary solvent mixture.

It was observed that, in all cases except for the above-mentioned diorite sample DGSb, the uncoated surfaces cleaned by the solvent mixtures showed lower static contact angle values compared to the surfaces coated with anti-graffiti product, regardless of the protective coating composition.

Considering the surfaces coated with anti-graffiti, the gneiss and travertine samples coated with the permanent anti-graffiti product showed lower values for the static contact angle than the samples coated with the sacrificial anti-graffiti product. For the granite and diorite samples, the situation was reversed: the surfaces coated with the permanent anti-graffiti product showed higher values than the surfaces with the sacrificial coating. However, in general, the values of the static contact angles for the coated surfaces with anti-graffiti products were very close.

SEM observations allowed the identification of both graffiti remains after cleaning and the presence of anti-graffiti products on the surfaces.

Figure 9 shows SEM micrographs and EDX spectra of the uncoated surfaces, cleaned with the low-toxic ternary solvent mixture A or B. EDX maps of the Ti distribution are also added for some of the micrographs: in these cases, the presence of TiO_2 nanoparticles used as extenders and opacifiers for the paints [54] can be used as a marker to identify the presence of graffiti remains. Despite the lowest intensity in the EDX spectra, Cl can also be used as a marker of graffiti remains.

On the silicate stones (Figure 9, GnVSa, GnGSa, GVSa, and GGSa), graffiti remains were mainly detected in the characteristic transgranular, intergranular, and intragranular fissures [51], while in the case of the travertine (Figure 9, TVSb and TGSb), they were mainly located in the voids. Due to the higher roughness related to the flamed surface finish, a greater accumulation of paint, no matter whether violet or green, was found in the fissures of the gneiss, if compared to the polished granite and diorite (Figure 9, GnVSa and GnGSa).

Moreover, two different patterns were identified for the paint remains (Figure 9, GnGSa and GVSa with the respective EDX spectra): (i) deposits with a lower contrast in BSE mode and high C content (Figure 9 EDX 2) and (ii) nanoparticle accumulation with a high contrast in BSE mode and high Ti content; to a lesser extent, Cl was identified in the respective EDX spectra of the two graffiti paints (Figure 9 EDX 1 and 3). Considering the silicate stones, the C-rich deposits were more abundant on surfaces with a higher roughness (gneiss) than on the smoother ones (granite and diorite). The latter were demonstrated to be richer in terms of Ti nanoparticle accumulation (Figure 9, GGSa and the respective Ti-map). As for the travertine, C-rich deposits were found in the void typical of this stone (Figure 9, TVSb), but accumulations of Ti nanoparticles were also identified on the surface (Figure 9, TVSb and the respective Ti map and TGSb).

Figures 10 and 11 show SEM micrographs of the surfaces coated with the sacrificial and permanent anti-graffiti products, respectively, after cleaning; EDX spectra are also reported. As already highlighted by stereomicroscopy, SEM observations confirmed the presence of the lowest amount of graffiti remains on the surfaces with anti-graffiti (Figures 10 and 11) compared to the uncoated surfaces (Figure 9), except for the case of the surfaces coated with the permanent anti-graffiti product and painted with violet spray (GVP, DVP, GnVP, and TVP). For these samples, the cleaning treatment proved to be ineffective, leaving the surface totally covered by the violet paint layer. Therefore, in these cases, SEM-EDX was obviously not necessary to observe the presence of the violet paint, but the analyses were performed anyway, in order to observe the morphology of the paint layer and any possible effect of the action of the graffiti remover on it.
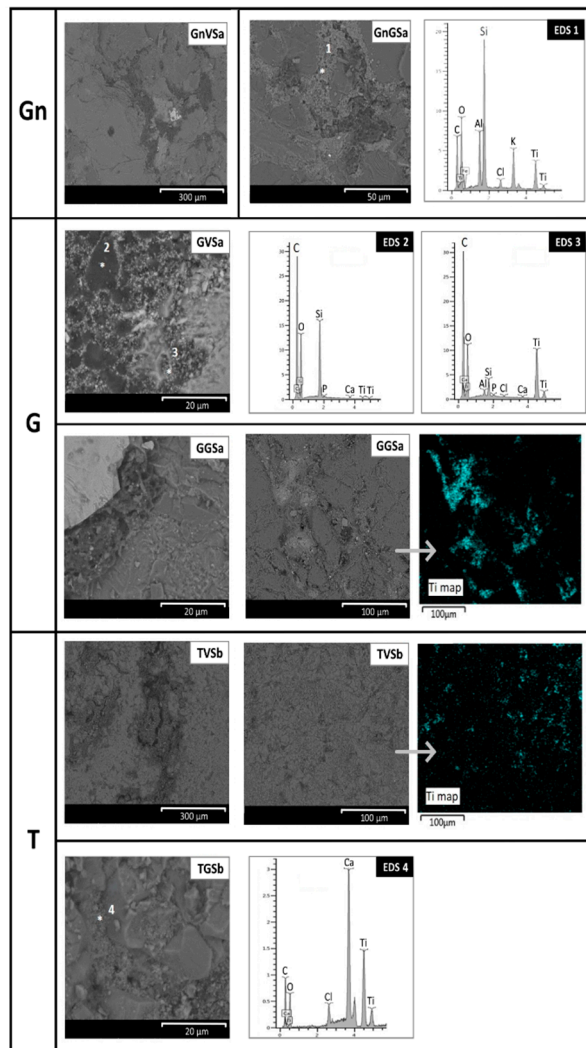
Figure 9. SEM micrographs, EDX spectra, and Ti-maps collected of the stones cleaned with the low-toxic ternary solvent mixture. Check Table 1 for sample labeling.
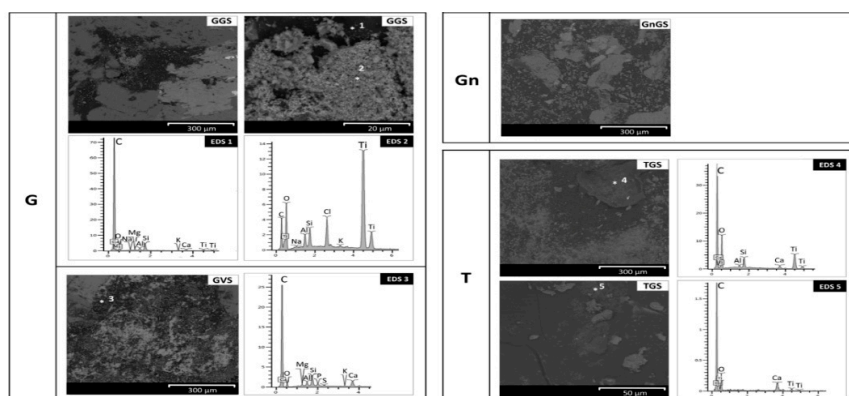

Figure 10. SEM micrographs and EDX spectra of the stones coated with the sacrificial anti-graffiti product after being cleaned with the product recommended by the manufacturer. Check Table 1 for sample labeling.
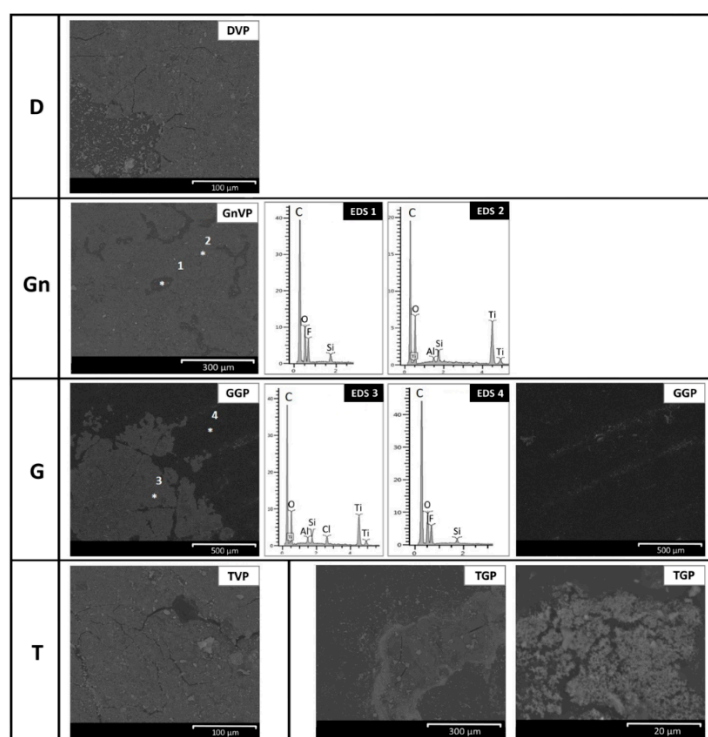
Figure 11. SEM micrographs and EDX spectra of the stones coated with the permanent anti-graffiti product after being cleaned with the product recommended by the manufacturer. Check Table 1 for sample labeling.

On the surfaces coated with the sacrificial anti-graffiti product, the SEM analyses confirmed the information already provided by the UV reflected photographs: although it was supposed to be removed along with the graffiti paint layer, numerous remains of the protective coating were present on the surface after that the cleaning treatment with the remover recommended by the manufacturer was performed (Figure 10, GGS, GVS, GnGS, and TGS). In fact, under large remains of paint with Ti-rich EDX spectra, the presence of the anti-graffiti product was highlighted, thanks to the EDX spectra showing an intense C peak, matching the organic composition (wax) of this anti-graffiti product (Figure 10, EDX 1 and 2).

Regarding the surfaces coated with the permanent anti-graffiti product, the cleaning treatment did not allow the removal of the violet graffiti paint from any of the lithotypes, as already reported (Figure 11, DVP, GnVP, and TVP). However, despite the violet paint layer being unaffected by the application of the commercial graffiti remover upon a visual observation with the stereomicroscope, the SEM analyses highlighted fissures and cracks in the paint layer, possibly showing the initial step of the detaching process from the protective coating (Figure 11, DVP and TVP). The permanence of this anti-graffiti product on the stone surface after cleaning was confirmed by the presence of an almost continuous layer, characterized by C- and F-rich EDX spectra (Figure 11, EDX 1, EDX 4); however, gaps and lacunas in the protective layer were observed. For samples painted with the green graffiti, some graffiti paint remains were identified on the surfaces (Figure 11, GGP and TGP), although in smaller quantities than for the samples painted with the violet spray (Figure 11, GGP and TGP) or for the same graffiti paint applied on uncoated stones (Figure 9, GnGSa, GGSa, and TGSb). Such as was reported for the cleaning of surfaces coated with the sacrificial anti-graffiti product, the green paint remains showed two different patterns: (i) C-rich deposits and (ii) an accumulation of Ti nanoparticles exhibiting agglomerations (Figure 11, TGP).

4. Discussion

In this research, the effectiveness of two anti-graffiti products for the protection of ornamental stones employed in architecture was tested. The two protective coatings considered are different in terms of their chemical composition and functioning: one is a ready-to-use sacrificial product, composed of an aqueous dispersion of microcrystalline wax; the other one is a bicomponent permanent anti-graffiti, composed of a fluorinated polyurethane in a water emulsion. The two anti-graffiti products were applied on four lithotypes, selected from the large variety of stones present in the architecture of the city center of Turin (NW Italy). These lithotypes were different in terms of their texture, mineralogy, and surface finish: polished Baveno granite and Vico diorite, an orthogneiss (Luserna Stone) with a flamed surface, and a travertine with a disc-cutting smooth surface. The coated samples were painted with two graffiti products, consisting of an alkyd-based violet paint and an acrylic-based green paint, and then cleaned by using two commercial removers recommended for each of the two anti-graffiti products by the manufacturers. For comparison purposes, the two graffiti paints were also applied on uncoated stone surfaces (without anti-graffiti product) and they were cleaned by means of a low-toxic ternary solvent mixture, composed of ethyl alcohol, acetone, and 2,2,4-trimethylpentane. The % concentration for each solvent was calculated by using the open source software Trisolv® [55], based on the triangular Teas graph [45,46], and taking into account the final purpose of keeping the same solubility parameters of two organic solvents, methyl ethyl ketone (MEK) and n-butyl acetate, which were used in [13] and exhibited satisfactory cleaning effectiveness levels in preliminary cleaning tests. Despite their common use in the field of restoration, these two solvents are quite toxic, since their TLV-TWA values are 200 and 50 ppm, respectively [43]. Therefore, n-butyl acetate was replaced by mixture A (51% ethyl alcohol, 11% acetone, and 38% 2,2,4-trimethylpentane) and MEK by mixture B (7% ethyl alcohol, 80% acetone, and 13% 2,2,4-trimethylpentane). As was stated in [13], depending on the surface roughness and the paint–stone interaction, mixture A produced the best results for granite and diorite samples, while mixture B provided the best performance for gneiss and travertine surfaces.

Comparing the results achieved for coated and uncoated samples, it was noticed that both the anti-graffiti and paint compositions and the interaction between them had a remarkable influence on the performance of each anti-graffiti product; although, to a lesser extent, the stone properties (mineralogy, texture, and surface finish) also affected the performance of the anti-graffiti product. This is not surprising and is actually in accordance with what was reported by other authors. For example, Carmona-Quiroga et al. [7] confirmed that the roughness associated with the surface finish is a key factor for the protection effectiveness ensured by a permanent fluorinated siloxane anti-graffiti product on stones. Indeed, the highest effectiveness of the anti-graffiti product, even after several painting–cleaning cycles, was achieved in the case of a smooth limestone rather than for an unpolished granite.

Furthermore, regardless of the lithotype, paint, and anti-graffiti product, the stereomicroscopy and SEM-EDX analyses allowed us to identify two types of graffiti remains, recognizable in terms of their morphology and composition: (i) C-rich deposits, which can be voluminous or filling fissures, and (ii) Ti nanoparticles agglomerations filling surface irregularities. On the one hand, since the graffiti paints considered are characterized by the presence of organic pigments, it can be concluded that the former deposits are responsible for the visible paint remains on the surface. On the other hand, the latter are due to the addition of TiO_2 nanoparticles as opacifiers [54,56]. These Ti nanoparticle agglomerations are white or colorless powders, with a very low solubility in water and preferably inert to the action of acids and alkalis [56]. The use of Ti as a marker element to detect the presence of graffiti remains has already been applied in previous works [16,20]. However, in the cited references, these remains were notably lower (amount and extension) than those registered in this research because the cleaning procedures were different: laser and mechanical methods. A laser [20] heats the material, which is consequently evaporated or sublimated, and mechanical procedures induce the removal of graffiti on the stone by abrading the surfaces. However, the chemical methods used in this research to clean graffiti, regardless of anti-graffiti coatings, are based on the application of solutions which react with the organic paint phases (pigment and binder) and dissolve them, leaving the inert compounds

(extenders) susceptible to being extracted by the brush. Therefore, the chemical product used for the cleaning (either the low-toxic ternary solvent mixture or one of the two commercial graffiti removers) dissolved the organic phase of the paint and induced an enrichment in the TiO_2 nanoparticles, which exhibited colloidal behavior [57]. As a consequence of the dissolution of the paints, their penetration through the fissures and a ghosting effect occurred, mainly on the silicate stones (granite, diorite, and gneiss) [12,13].

Considering the sacrificial anti-graffiti product tested (microcrystalline wax), an enhancement of the graffiti removal was detected, regardless of the paint. In fact, for both the violet and green painted samples, a satisfactory cleaning level was achieved by applying the specific graffiti remover (mixture of alkyl carbonate, ethyl pyrrolidone, alcohol ethoxylates, and dimethyl adipate) on the surface with a brush, even though the presence of a few graffiti remains was observed in fissures after the cleaning. Unlike in Pozo-Antonio et al. [11], who worked with granite samples coated with a permanent fluoralkyl siloxane and a sacrificial water-based crystalline micro wax, the cleaning effectiveness on polished granite and diorite did not seem to be remarkably affected by the grain size. This mismatching may be related to the surface finish and the weathering of the stone: within this work, the substrates were unweathered and the surface polishing reduced the penetration of the graffiti, even on samples without anti-graffiti product. Conversely, in Pozo-Antonio et al. [11], one of the granites showed a high weathered condition, with the presence of higher fissuring retaining the graffiti paints.

For surfaces coated with the permanent anti-graffiti product (fluorinated polyurethane), two behaviors were observed, depending on the graffiti paint composition:

- The removal of the green acrylic paint was satisfactory from all four stones. Nevertheless, as for the samples with sacrificial anti-graffiti product, paint remains filling the voids were found on travertine surfaces. Therefore, the commercial graffiti remover employed (a blend of alcohol and terpene solvents) proved to be effective in the dissolution of this paint;
- The cleaning of the violet alkyd paint was totally unsatisfactory, leaving the graffiti layer apparently unaffected. However, an observation by SEM revealed a few fissures and cracks in the paint layer, possibly showing the initial step of the detaching process from the protective coating.

When evaluating the surfaces cleaned with the solvent mixtures, different results were obtained, depending on the stone underneath and its texture and surface finish. For the polished stones, granite and diorite, good cleaning results were achieved; however the ghosting effect was observed. Conversely, for gneiss and travertine samples, the paint removal was definitely less encouraging. Although the graffiti paint composition did not dramatically influence the cleaning effectiveness of the solvent mixtures, it was noticed that, mainly on the polished surfaces, the green acrylic seemed to be more difficult to remove than the violet alkyd paint, resulting in a higher amount of graffiti remains being identified by stereomicroscopy. However, greater amounts of graffiti remains were found overall on the roughest substrate considered (the gneiss), in the fissures and the surface irregularities derived from the flaming procedure applied as a surface finish. For the travertine, despite its smooth disc-cutting surface, the permanence of paint remains in the characteristic voids hindered the cleaning effectiveness; C-rich deposits were identified in the voids, while Ti nanoparticle accumulation was found around the rhombohedral calcite grains. Therefore, the surface finish and consequently the roughness seemed to be key factors explaining the amount of graffiti remains on the stone [16].

Concerning the physical properties evaluated (roughness, water absorption, and static contact angle) on both the coated and uncoated surfaces after cleaning treatments, different trends were obtained.

With regard to the roughness measurements, a decrease of the R_{3z} values was observed after the cleaning in the case of the gneiss samples coated with either of the two anti-graffiti products. In particular, the decrease of roughness was due (i) to the permanence of both anti-graffiti and graffiti paint remains in fissures, for all surfaces coated with the sacrificial anti-graffiti product; (ii) to the presence of the permanent anti-graffiti product on samples painted with the green graffiti (considering that very few paint remains were found on those samples identified by SEM-EDX); and (iii) finally, to

the violet paint layer, which could not be removed by using the commercial remover on the samples coated with the permanent anti-graffiti product.

In the case of both the polished substrates (diorite and granite) and the disc-cutting surfaces (travertine), variations of the roughness without a clear trend were detected, suggesting different situations: (i) the permanence of voluminous deposits associated with remains of either paint or sacrificial anti-graffiti product induced an increase of the roughness, while, (ii) on the contrary, the presence of both graffiti and anti-graffiti products in the fissures and voids caused a decrease of the roughness, as already observed by Pozo-Antonio et al. [11].

Finally, considering the surfaces cleaned with the solvent mixtures, although a limited impact on the original surfaces seemed to be exerted, the roughness was clearly influenced by the presence of graffiti remains detected by stereomicroscopy.

Considering the water absorption and static contact angle after cleaning, it was generally observed that the coated surfaces, regardless of the anti-graffiti product and paint applied, showed lower water absorption and a higher static contact angle if compared to the reference stones. The contact angle values were higher than 90°, showing hydrophobic behavior [52], similar to what was reported in [11] for granite surfaces coated with a permanent water-based fluoralkyl siloxane. Instead, the static contact angles of the stone references displayed hydrophilic behavior, since their contact angles were lower than 90°. The contact angle values acquired within the present work were in accordance with those obtained by Carmona-Quiroga et al. [7], who tested a fluorinated siloxane anti-graffiti product on a granite and limestone and, in the same way, suggested a decrease of the water absorption.

On the one hand, for samples coated with the sacrificial anti-graffiti product and painted with either the violet or green graffiti, the reduction of the water absorption and the increase of the static contact angle after the cleaning can be explained by the permanence of some remains of both the paint and the anti-graffiti product on the surface. The same is observed due to the presence of remains of the permanent coating after the cleaning of samples painted with green graffiti. Finally, a similar trend can be explained in the case of the samples coated with the permanent anti-graffiti product and painted with the violet spray, since the violet layer could not be removed.

Concerning the uncoated samples cleaned with the solvent mixtures, several graffiti remains filling the fissures could be responsible for a decrease of the water absorption and, in parallel, for a slight increase of the static contact angle (around 90°: hydrophobic behavior [52]). Among these surfaces, the most relevant decrease of water absorption was detected for samples with the violet paint. However, the observation made by stereomicroscopy allowed us to identify more visible remains of green paint rather than violet paint, thus suggesting that the variation in the water absorption is related to the Ti-rich colorless deposits in the fissures. Further studies should be performed considering the influence of those TiO_2 nanoparticles on the water absorption and hydrophobicity of the stones after being exposed to cleaning treatments.

A global assessment of cleaning methods applied in the field of Cultural Heritage should consider, on the one hand, the effectiveness of graffiti removal, and on the other hand, the alterations induced on the stone surfaces. Therefore, it is important to highlight that, after the application of anti-graffiti products, some visual changes to the stone surface were observed from the beginning. For instance, it was observed that the voids in the porous travertine were filled, regardless of the anti-graffiti composition; moreover, the application of the permanent anti-graffiti product on the polished surfaces, mainly on the diorite, created a layer with a milky appearance.

Additionally, considering the conservation guidelines stated by the Venice charter [58], although a sacrificial anti-graffiti product may be preferred because of its supposed reversibility, this did not occur in the present study: indeed, the cleaning product did not allow the complete removal of the coating together with the paint layers, leaving numerous wax remains on the surface, as detected by SEM-EDX and UV fluorescence photography. On the contrary, the permanent anti-graffiti layer was not continuous on the surfaces after one cleaning treatment, even though the manufacturer recommendations state that the product should resist up to 10 cycles. This may increase the risk of

ghosting and partial penetration of the paint in the substrate, after partial dissolution obtained during the cleaning treatment.

5. Conclusions

The application of anti-graffiti products to ornamental stones employed in architectural heritage has been proven to be a worthwhile procedure in specific conditions. Comparing the results of cleaning procedures achieved on surfaces with and without protective coatings, the effectiveness of both a sacrificial and permanent anti-graffiti product was tested on four different stones commonly found in the historical city center of Turin (Italy).

Regardless of the paint composition, the sacrificial anti-graffiti product enhanced the cleaning effectiveness in all cases; the main drawbacks highlighted were related to the presence of numerous anti-graffiti remains on the surface after cleaning. On the contrary, the effectiveness of the permanent anti-graffiti product proved to be paint-dependent, since the coating created an interaction with one of the graffiti paints, forming a single thick and insoluble layer. Moreover, some other drawbacks were highlighted in relation to the permanent coating durability. The results obtained in this research pointed out the importance of a careful selection of the most appropriate anti-graffiti product, considering the stone (mainly its texture, mineralogy, and surface finish) and the composition of the graffiti paints commonly used by the writers. Therefore, a specific survey carried out prior to anti-graffiti application can be very useful.

References

1. United Nations. About the Sustainable Development Goals (Agenda 2030). Available online: https://www.un.org/sustainabledevelopment/sustainable-development-goals (accessed on 20 March 2020).
2. Hosagrahar, J.; Soule, J.; Fusco Girard, L.; Potts, A.; ICOMOS. Concept Note for the United Nations Agenda 2030 and the Third United Nations Conference on Housing and Sustainable Urban Development (HABITAT). Available online: http://www.usicomos.org/wp-content/uploads/2016/05/Final-Concept-Note.pdf (accessed on 20 March 2020).
3. Sanmartín, P.; Cappitelli, F.; Mitchell, R. Current methods of graffiti removal: A review. *Constr. Build. Mater.* **2014**, *71*, 363–374. [CrossRef]
4. Pozo-Antonio, J.S.; Rivas, T.; Fiorucci, M.P.; López, A.J.; Ramil, A. Effectiveness and harmfulness evaluation of graffiti cleaning by mechanical, chemical and laser procedures on granite. *Microchem. J.* **2016**, *125*, 1–9. [CrossRef]

5. Gomes, V.; Dionísio, A.; Pozo-Antonio, J.S. Conservation strategies against graffiti vandalism on cultural heritage stones: Protective coatings and cleaning methods. *Prog. Organ. Coat.* **2017**, *113*, 90–109. [CrossRef]

6. Lettieri, M.; Masieri, M. Surface characterization and effectiveness evaluation of anti-graffiti coatings on highly porous stone materials. *Appl. Surf. Sci.* **2014**, *288*, 466–477. [CrossRef]

7. Carmona-Quiroga, P.M.; Martínez-Ramírez, S.; Blanco-Varela, M.T. Fluorinated anti-graffiti coating for natural stones. *Mater. De Constr.* **2008**, *58*, 233–246.

8. Carmona-Quiroga, P.M.; Rubio, J.; Sánchez, M.J.; Martínez-Ramírez, S.; Blanco-Varela, M.T. Surface dispersive energy determined with IGC-ID in anti-graffiti-coated building materials. *Prog. Organ. Coat.* **2011**, *71*, 207–212. [CrossRef]

9. Carmona-Quiroga, P.M.; Jacobs, R.M.J.; Martínez-Ramírez, S.; Viles, H.A. Durability of anti-graffiti coatings on stone: Natural vs. accelerated weathering. *PLoS ONE* **2017**, *12*, e0172347. [CrossRef]

10. Licchelli, M.; Malagodi, M.; Weththimuni, M.; Zanchi, C. Anti-graffiti nanocomposite materials for surface protection of a very porous stone. *Appl. Phys. A Mater. Sci. Process.* **2014**, *116*, 1525–1539. [CrossRef]

11. Pozo-Antonio, J.S.; Rivas, T.; Jacobs, R.M.J.; Viles, H.A.; Carmona-Quiroga, P.M. Effectiveness of commercial anti-graffiti treatments in two granites of different texture and mineralogy. *Prog. Organ. Coat.* **2018**, *116*, 70–82. [CrossRef]

12. Urquhart, D. *The Treatment of Graffiti on Historic Surfaces: Advice on Graffiti Removal Procedures, Anti-Graffiti Coatings and Alternative Strategies*; Historic Scotland technical advice note no.18; TCRE Division/Scottish Conservation Bureau, Hist.: Edinburgh, Historic Scotland, UK, 1999.

13. Giusti, C.; Colombini, M.P.; Lluveras-Tenorio, A.; la Nasa, J.; Striova, J.; Salvadori, B. Graphic vandalism: Multi-analytical evaluation of laser and chemical methods for the removal of spray paints. *J. Cult. Herit.* **2020**. [CrossRef]

14. Ortiz, P.; Antúnez, V.; Ortiz, R.; Martín, J.M.; Gómez, M.A.; Hortal, A.R.; Martínez-Haya, B. Comparative study of pulsed laser cleaning applied to weathered marble surfaces. *Appl. Surf. Sci.* **2013**, *283*, 193–201. [CrossRef]

15. Carvalhão, M.; Dionísio, A. Evaluation of mechanical soft-abrasive blasting and chemical cleaning methods on alkyd-paint graffiti made on calcareous stones. *J. Cult. Herit.* **2015**, *16*, 579–590. [CrossRef]

16. Pozo-Antonio, J.S.; López, L.; Dionísio, A.; Rivas, T. A Study on the suitability of mechanical soft-abrasive blasting methods to extract graffiti paints on ornamental stones. *Coatings* **2018**, *8*, 335. [CrossRef]

17. Rivas, T.; Pozo, S.; Fiorucci, M.P.; López, A.J.; Ramil, A. Nd: YVO4 laser removal of graffiti from granite. Influence of paint and rock properties on cleaning efficacy. *Appl. Surf. Sci.* **2012**, *263*, 563–572. [CrossRef]

18. Samolik, S.; Walczak, M.; Plotek, M.; Sarzynski, A.; Pluska, I.; Marczak, J. Investigation into the removal of graffiti on mineral supports: Comparison of nanosecond Nd:YAG laser cleaning with traditional mechanical and chemical methods. *Stud. Conserv.* **2015**, *60*, S58–S64. [CrossRef]

19. Atanassova, V. Laser cleaning of graffiti spray paints on marble, limestone and granite. In *Graffiti: Vandalism, Street Art and Cultural Significance*; Paradis, X., Matthew, M., Eds.; Nova Science Publishers: New York, NY, USA, 2018; pp. 117–144.

20. Pozo-Antonio, J.S.; Papanikolaou, A.; Melessanaki, K.; Rivas, T.; Pouli, P. Laser-assisted removal of graffiti from granite: Advantages of the simultaneous use of two wavelengths. *Coatings* **2018**, *8*, 124. [CrossRef]

21. Sanmartín, P.; DeAraujo, A.; Vasanthakumar, A.; Mitchell, R. Feasibility study involving the search for natural strains of microorganisms capable of degrading graffiti from heritage materials. *Int. Biodeterior. Biodegrad.* **2015**, *103*, 186–190. [CrossRef]

22. Sanmartín, P.; Bosch-Roig, P. Biocleaning to remove graffiti: A real possibility? Advances towards a complete protocol of action. *Coatings* **2019**, *9*, 104. [CrossRef]

23. Macchia, A.; Ruffolo, S.A.; Rivaroli, L.; Malagodi, M.; Licchelli, M.; Rovella, N.; Randazzo, L.; la Russa, M.F. Comparative study of protective coatings for the conservation of urban art. *J. Cult. Herit.* **2020**, *41*, 232–237. [CrossRef]

24. García, O.; Rz-Maribona, I.; Gardei, A.; Riedl, M.; Vanhellemont, Y.; Santarelli, M.L.; Suput, J.S. Comparative study of the variation of the hydric properties and aspect of natural stone and brick after the application of 4 types of anti-graffiti. *Mater. De Constr.* **2010**, *60*, 69–82. [CrossRef]

25. Carmona-Quiroga, P.M.; Martínez-Ramírez, S.; Sánchez-Cortés, S.; Oujja, M.; Castillejo, M.; Blanco-Varela, M.T. Effectiveness of anti-graffiti treatments in connection with penetration depth determined by different techniques. *J. Cult. Herit.* **2010**, *11*, 297–303. [CrossRef]

26. Grossi, D.; del Lama, E.A. Avaliação da eficácia de hidrofugantes e anti-graffiti no arenito itararé. geologia USP. *Série Cient.* **2018**, *18*, 43–55. [CrossRef]

27. Moura, A.R.; Flores-Colen, I.; de Brito, J. Analysis of graffiti removal techniques and anti-graffiti products for porous materials. In Proceedings of the Hydrophobe VII—7th International Conference on Water Repellent Treatment and Protective Surface Technology for Building Materials, Lisboa, Portugal, 11–12 September 2014.

28. García, O.; Malaga, K. Definition of the procedure to determine the suitability and durability of an anti-graffiti product for application on cultural heritage porous materials. *J. Cult. Herit.* **2012**, *13*, 77–82. [CrossRef]

29. Gardei, G.; Garcia, O.; Riedl, M.; Vanhellemond, I.; Suput, J.S.; Santarelli, M.L.; Rodriguez-Maribona, I.; Müller, U. Performance and durability of a new anti-graffiti system for cultural heritage–The EC project GRAFFITAGE. In Proceedings of the 11th International Congress on Conservation and Deterioration of Stone, Torun, Poland, 15–20 September 2008; pp. 889–897.

30. Ricci, C.; Gambino, F.; Nervo, M.; Piccirillo, A.; Scarcella, A.; Zenucchini, F.; Pozo-Antonio, J.S. Developing new cleaning strategies of cultural heritage stones: Are synergistic combinations of a low-toxic solvent ternary mixtures followed by laser the solution? *Coatings* **2020**, *10*, 466. [CrossRef]

31. Gambino, F.; Borghi, A.; D'Atri, A.; Gallo, L.M.; Ghiraldi, L.; Giardino, M.; Martire, L.; Palomba, M.; Perotti, L. TOURinSTONES: A free mobile application for promoting geological heritage in the city of Turin (NW Italy). *Geoheritage* **2018**, *11*, 3–17. [CrossRef]

32. Borghi, A.; Cadoppi, P.; Dino, G.A. The dora-maira unit (Italian cottian alps): A reservoir of ornamental stones locally and worldwide employed since Roman age. In *EGU General Assembly Conference Abstracts*; European Geosciences Union General Assembly: Vienna, Austria, 2015; Volume 17.

33. Berra, V.; Borghi, A.; Gallo, L.M. I portici di via Roma a Torino: Rilievo architettonico e caratterizzazione petrografica. *Riv. Piemont. Di Stor. Nat.* **2013**, *34*, 3–80.

34. Poretti, G.; Borghi, A.; Dino, G.A.; Ferrando, S.; Groppo, C.; Martire, L.; Accattino, E.; Favero Longo, S.E.; Piervittori, R.; Rolfo, F. The stone bridges on the Po River at Turin (NW Italy): A scientific dissemination approach for the development of urban geological heritage. In *Engineering Geology for Society and Territory*; Springer: Cham, Switzerland, 2015; Volume 8, pp. 207–211.

35. Cavallo, A.; Bigioggero, B.; Colombo, A.; Tunesi, A. The verbano cusio ossola province: A land of quarries in northern Italy (Piedmont). *Period. Mineral.* **2004**, *73*, 197–210.

36. Boriani, A.; Burlini, L.; Caironi, V.; Origoni, E.G.; Sassi, A.; Sesana, E. Geological and petrological studies on the hercynian plutonism of serie dei laghi–geological map of its occurrence between Valsesia and Lago Maggiore (N-Italy). *Rend. Soc. It. Mineral. Petrol.* **1988**, *43*, 367–384.

37. Natural Stone Institute. Restoration and Maintenance. In *An Excerpt from the Dimension Stone Design Manual, version VIII*; Marble Institute of America: Oberlin, OH, USA, 2016; 123p.

38. Sandrone, R.; Colombo, A.; Fiora, A.; Fornaro, L.; Lovera, E.; Tunesi, A.; Cavallo, A. Contemporary natural stones from the Italian western Alps (Piedmont and Aosta Valley Regions). *Per. Mineral.* **2004**, *73*, 211–226.

39. Ciriaco, G.; Aldega, L. *Il travertino: La Pietra di Roma*; Società Geologica Italiana: Roma, Italy, 2013; Volume 27, pp. 98–109.

40. Available online: www.san-marco.com (accessed on 31 January 2018).

41. Available online: www.docchem.com (accessed on 31 January 2018).

42. Available online: www.montanacolors.com (accessed on 31 January 2018).

43. U.S. National Library of Medicine. National Center for Biotechnology Information. Available online: https://pubchem.ncbi.nlm.nih.gov (accessed on 31 January 2018).

44. TriSolv Software, ISCR. Triangolo Interattivo dei Solventi e Delle Solubilità®. Available online: http://icr.beniculturali.it/flash/progetti/TriSolv/TriSolv.html (accessed on 31 January 2018).

45. Cremonesi, P. *L'uso dei Solventi Organici Nella Pulitura di Opere Policrome*; Il Prato: Villatora, Italy, 2004.

46. Kanegsberg, B.; Kanegsberg, E. (Eds.) *Handbook for Critical Cleaning: Cleaning Agents and Systems*; CRC Press: Cleveland, OH, USA, 2011.

47. UNI 11432:2011. *Beni Culturali—Materiali Lapidei Naturali ed Artificiali—Misura della Capacità di Assorbimento di Acqua Mediante Spugna di Contatto*; Ente Italiano di Normazione: Rome, Italy, 2011; Available online: http://store.uni.com/catalogo/uni-11432-2011?josso_back_to=http://store.uni.com/josso-security-check.php&josso_cmd=login_optional&josso_partnerapp_host=store.uni.com (accessed on 21 June 2020).

48. Vandevoorde, D.; Pamplona, M.; Schalm, O.; Vanhellemont, Y.; Cnudde, V.; Verhaeven, E. Contact sponge method: Performance of a promising tool for measuring the initial water absorption. *J. Cult. Herit.* **2009**, *10*, 41–47. [CrossRef]

49. BS, EN. 828. *Adhesives. Wettability. Determination by Measurement of Contact Angle and Surface Free Energy of Solid Surface*; European Committee for Standardization: Brussels, Belgium, 2013.

50. UNI-EN; ISO. Surface texture: Profile method, terms, definitions and surface texture parameters. In *ISO 4288, Geometrical Product Specifications (GPS)*; Ente Italiano di Normazione: Rome, Italy, 1999.

51. Mosquera, M.J.; Rivas, T.; Prieto, B.; Silva, B. Capillary rise in granitic rocks: Interpretation of kinetics on the basis of pore structure. *J. Colloid Interface Sci.* **2000**, *222*, 41–45. [CrossRef] [PubMed]

52. Bico, J.; Thiele, U.; Quéré, D. Wetting of textured surfaces. *Colloids Surf. A Physicochem. Eng. Asp.* **2002**, *206*, 41–46. [CrossRef]

53. de Gennes, P.G. Wetting: Statics and dynamics. *Rev. Mod. Phys.* **1985**, *57*, 827–863. [CrossRef]

54. Abel, A. Pigments for paints. In *Paints in Surface Coatings: Theory and Practice*; Lambourne, R., Strivens, T.A., Eds.; Woodhead Publishing: Cambridge, UK, 1999.

55. Coladonato, M.; Scarpitti, P. Note sul Triangolo Interattivo dei Solvent e Delle Solubilità ©. 2008. Available online: http://www.icr.beniculturali.it/flash/progetti/TriSolv/dati/IT/TriSolv_IT.pdf (accessed on 31 January 2018).

56. Marrion, A. *The Chemistry and Physics of Coatings*; The Royal Society of Chemistry: London, UK, 2004; 396p, ISBN 0-85404-656-9.

57. Al-Kattan, A.; Wichser, A.; Zuin, S.; Arroyo, Y.; Golanski, L.; Ulrich, A.; Nowack, B. Behavior of TiO_2 released from nano-TiO_2-containing paint and comparison to pristine nano-TiO_2. *Environ. Sci. Technol.* **2014**, *48*, 6710–6718. [CrossRef] [PubMed]

58. Charter, V. The Venice Charter for the Conservation and Restoration of Monuments and Sites. 1964. Available online: http://www.icomos.org/venicecharter2004/index.html (accessed on 31 January 2018).